J. Chem. Sci. (2020)132:65
https://doi.org/10.1007/s12039-020-01766-5

REGULAR ARTICLE

A molecular electron density theory study to understand the interplay of theory and experiment in nitrone-enone cycloaddition

NIVEDITA ACHARJEE[a,*] and AVIJIT BANERJI[b]
[a]Department of Chemistry, Durgapur Government College, Durgapur, West Bengal 713214, India
[b]Department of Chemistry, National Institute of Ayurvedic Drug Development, Salt Lake, Kolkata, West Bengal, India
E-mail: nivchem@gmail.com

MS received 29 October 2019; revised 16 December 2019; accepted 24 December 2019

Abstract. [3 + 2] cycloaddition (32CA) reaction of *C*,*N*-diaryl nitrone with benzylidene acetone has been studied to analyse the mechanism, selectivity and polar character of this nitrone-enone cycloaddition. Topological analysis of the electron localization function (ELF) shows the absence of *pseudoradical* and carbenoid centre in the nitrone, which allows its classification as a zwitter-ionic (*zw*) *type* three atom component (TAC) and hence participation in *zw- type* cycloadditions is associated with high activation energy barriers. This 32CA reaction follows a *one-step* mechanism with asynchronous TSs. *Endo/meta* product is obtained as the major cycloadduct experimentally, which can be rationalized from its calculated lowest activation energy among the four possible reaction pathways. Global electron density transfer (GEDT) at the TSs predict the non-polar character of this 32CA reaction. Topological analysis of the ELF and QTAIM parameters was performed at the TSs. Finally, non-covalent interaction (NCI) gradient isosurfaces are computed to obtain a visualization of non-covalent interactions at the interatomic bonding regions.

Keywords. ELF; cycloaddition; transition state; QTAIM; MEDT.

1. Introduction

[3 + 2] cycloaddition (32CA) reactions[1,2] of nitrones to olefins have remained a versatile protocol for the synthesis of isoxazolidines since the last 40-50 years. Isoxazolidines with three contiguous stereocenters require special mention since they constitute a pivotal structural feature of biologically interesting compounds[3,4] and are also identified as valuable intermediates in important synthetic routes.[1,2] Numerous experimental studies devoted to 32CA reactions of nitrones and enones (Scheme 1) are documented in literature[5] and this reaction system is still receiving increased attention from synthetic organic chemists.[6]

Frontier Molecular Orbital (FMO) theory proposed by Fukui[7] in 1952 was considered as the only alternative for interpretation of organic reactions, until recently in 2016, a new outlook of organic reactivity, named as *Molecular Electron Density Theory* (MEDT) was proposed by Domingo,[8] stating that the changes in electron density are responsible for molecular reactivity. MEDT[8,9] has been extensively justified by the use of advanced computing software for the last three years. In 2017, Domingo[10] explained the role of electron density flux between reactants (global electron density transfer[11] (GEDT)) in decreasing activation energies of polar cycloadditions and concluded that electron density transfer between reactants facilitates the rupture of C-C double bonds and hence results in lowered activation energy of polar Diels Alder reactions. In a 2018 MEDT study, Domingo[12] explained the underlying reason behind high activation energies of non-polar 32CA reactions of nitrone-alkene systems compared to the corresponding polar 32CA reactions. Non-polar nitrone-alkene 32CA

*For correspondence

Electronic supplementary material: The online version of this article (https://doi.org/10.1007/s12039-020-01766-5) contains supplementary material, which is available to authorized users.

Published online: 23 April 2020

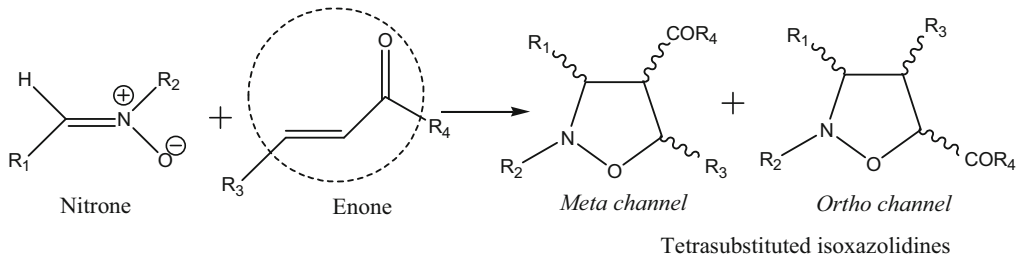

Scheme 1. 32CA of the nitrone-enone system leading to tetrasubstituted isoxazolidine.

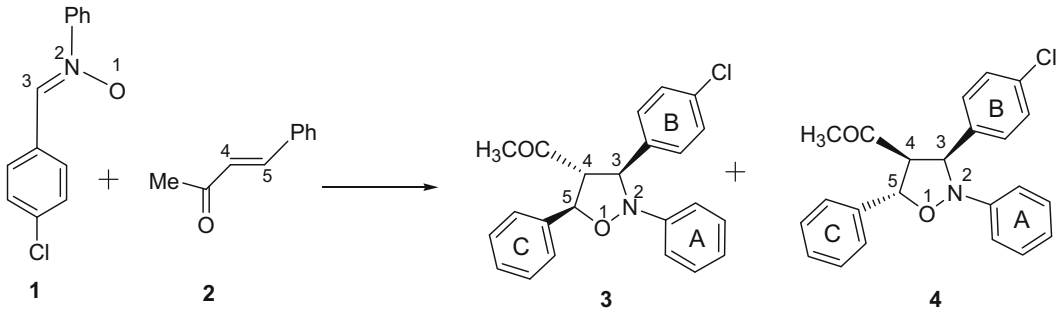

Scheme 2. 32CA reaction of *C*-(4-chlorophenyl)-N-phenyl nitrone (**1**) and Benzylidene acetone (**2**).

reactions involve the formation of new C-C single bond through the coupling of *pseudoradical* centers, while polar 32CA reactions involve the formation of new C-O single bond by donation of the nonbonding electron density by the nitrone oxygen. *Pseudoradical* centers are created in non-polar 32CA reactions by the rupture of the olefinic double bond, which requires high energy and hence accounts for the additional energy requirement of non-polar 32CA reactions compared to polar reactions. Now, enone systems (Scheme 1) have conjugated olefin-carbonyl framework which causes depopulation of the olefinic double bond and hence the role of such a framework in the energy requirement of 32CA reactions is worth investigating. With this in mind, the present MEDT study aims to analyse the mechanism and the origin of activation energy in 32CA reactions of enones. MEDT study for nitrone-enone system leading to tetrasubstituted isoxazolidine is studied for the first time in this paper. 32CA reaction between *C*-(4-chlorophenyl)-*N*-phenyl nitrone (**1**) and benzylidene acetone (**2**) is selected as the computational model (Scheme 2) for the present MEDT study.

This report has been divided into four sections. (1) Documentation of experimental findings (2) Electron localization function[13,14] (ELF) topological study and analysis of conceptual[15] (CDFT) indices at the ground state of the reagents (3) Study of the energy profile and ELF topological study at the TSs (4) Analysis of Quantum Theory of Atoms in Molecules[16–18] (QTAIM) parameters and NCI[19] gradient isosurfaces at the TSs.

2. Computational methods

Density functional theory (DFT) calculations were carried out using B3LYP functional[20,21] in conjunction with the standard 6-31G(d) basis set, which is identified as a precise computational level to study several 32CA reactions.[22–24] Stationary states on the potential energy surface were characterized through frequency calculations at the same level. The intrinsic reaction coordinate (IRC) pathways of the investigated CAs were traced using the second-order Gonzales-Schlegel integration method[25,26] to check that the energy profiles connect the two associated minima on the potential energy surface. Solvent effects of toluene were taken into account by single-point energy calculations of the gas phase structures using polarised continuum model[27,28] (PCM) in the framework of SCRF.[29,30] GEDT[11] values were calculated from natural bond orbital (NBO) calculations.[31,32] CDFT global reactivity indices,[15,33,34] electronic chemical potential (μ), global hardness (η), global electrophilicity (ω) and relative nucleophilicity N were calculated from the formula cited in reference 15.[15] Computational studies were performed using Gaussian 03 suite of programs (Revision D.01).[35] ELF topological studies and calculation of QTAIM parameters

was performed using Multiwfn[36] program. Non-covalent interactions[19] (NCIs) were analyzed through evaluation of the B3LYP/6-31G(d) monodeterminantal wave functions of the located transition states by using Multiwfn program.[36] ELF basin analysis was performed with a high-quality grid with spacing of 0.06 Bohr. ELF basins and attractors were visualized by using VMD software[37] and UCSF Chimera software.[38]

2.1 *Experimental methods*

Nitrone **1** was prepared by refluxing phenylhydroxylamine (prepared from nitrobenzene using zinc and ammonium chloride) and 4-chlorobenzaldehyde in ethanol in water bath for 2 h. Nitrone **1** separated as white crystals which were then recrystallized in ethanol. Benzylidene acetone **2** was obtained from the mixed aldol condensation of benzaldehyde and acetone.[39] Reactants **1** and **2** were obtained in pure form and confirmed by IR and NMR studies. For the cycloaddition reaction, 0.0044 mol of reactant **1** was allowed to react with 0.0066 mol of reactant **2** in 5 cm^3 refluxing dry thiophene-free toluene under a nitrogen atmosphere for 16 h. The cycloaddition was monitored by the examination of reaction aliquots at regular intervals of time by thin-layer chromatography (using benzene-ethyl acetate (4:1) solvent system and silica gel adsorbent) and 300 MHz ^{1}H spectroscopy. After completion of the run time, excess toluene was removed from the post-reaction mixtures under reduced pressure using a rotary evaporator. Cycloadducts were isolated from the crude reaction mixture by column chromatography over neutral alumina (Activity I-II, Merck) using petroleum ether and benzene mixtures as the eluents. The column was initially eluted with petroleum ether (bpt: 60-80 °C) and then progressively, the proportion of benzene was increased in the eluent. All starting materials and solvents used for reactions and chromatographic separation were distilled before use. IR spectra of the cycloadducts were recorded using a Perkin-Elmer RX-9 FT-IR spectrophotometer. ^{1}H and ^{13}C NMR spectra of the cycloadducts and crude reaction mixtures were recorded by a Bruker AV-300 NMR spectrometer at 300 and 75.5 MHz, respectively. Spectra were recorded in $CDCl_3$ solvent. Chemical shifts for NMR are reported in ppm, downfield from TMS. Mass spectra are recorded using a JEOL JMS600 H mass spectrometer.

2.1a *(3α,4β,5α)-3-(4-chlorophenyl)-4-oxomethyl-2,5-Diphenyl-isoxazolidine (**3**, $C_{23}H_{20}ClNO_2$)*: White amorphous solid, M.p.: 122 °C, 0.96 gm (58%), isolated from 10% benzene in petroleum ether (60-80 °C) eluates, R_f = 0.51 (silica gel, petroleum ether (60-80 °C) : benzene = 1:1), IR(cm^{-1})(KBr): $\bar{\nu}$ = 3077(w), 1670 (s), 1520 (s), 1347(s), 1251 (s), 827 (m), 752 (s), 692(s), ^{1}H NMR (300MHz, $CDCl_3$,):δ 5.58 (1H,d, J = 7.0 Hz, H3), 4.03 (1H,dd, J = 7.0, 9.2 Hz, H4), 5.46 (1H,d, J = 9.2 Hz, H5), 6.88 (3H, m H2,4,6 (A)), 7.08-7.31 (m, H3,5(A), H2,3,5,6 (B), H2,3,4,5,6 (C)), 2.29 (s, CH_3); ^{13}C NMR (75.5MHz, $CDCl_3$,): δ 74.28 (C3), 69.20 (C4), 84.78 (C5), 151.32 (C1(A)), 114.42 (C2,6(A)), 127.92 (C3,5(A)), 122.30 (C4(A)), 136.33, 136.89 (C1(B), C1(C)), 133.15(C4(B), 126.77 (C3,5(C)),128.95 (C4(C)), 128.77, 128.68, 128.43 (C2,6(B), (C3,5(B), C2,6(C)), 196.20 (C=O), 27.42 (-CH_3); MS: *m/z*377 ($C_{23}H_{20}NO_2Cl$, M^+), 242 ($C_{15}H_{11}OCl$), 231 ($C_{13}H_{10}NOCl$), 216 ($C_{13}H_{11}NCl$), 131 ($C_9H_7O^+$), 111 ($C_6H_4Cl^+$), 91 (C_7H_7+).

2.1b *(3α,4α,5β)-3-(4-chlorophenyl)-4-oxomethyl-2,5-Diphenyl-isoxazolidine (**4**, $C_{23}H_{20}ClNO_2$)*: White amorphous solid, 0.12 gm (7%), isolated from 20% benzene in petroleum ether (60-80 °C) eluates, R_f = 0.60 (silica gel, petroleum ether (60-80 °C) : benzene = 1:1), IR(cm^{-1})(KBr):$\bar{\nu}$ = 3045(w), 1677 (s), 1594 (s), 1487 (s), 825 (m), 755 (s), 695(s), ^{1}H NMR (300MHz, $CDCl_3$,):δ 5.35 (1H,d, J = 10.3 Hz, H3), 4.97 (1H,dd, J = 10.3, 9.1 Hz, H4), 6.51(1H,d, J = 9.1 Hz, H5), 6.93 (3H, m H2,4,6 (A)), 7.10-7.36 (m, H3,5(A), H2,3,5,6 (B), H2,3,4,5,6 (D)), 7.33-7.39 (m, H2,3,4,5,6 (C)), 2.18 (s, CH_3); ^{13}C NMR (75.5MHz, $CDCl_3$,): δ 73.48 (C3), 67.30 (C4), 84.75 (C5), 149.07 (C1(A)), 115.58 (C2,6(A)), 127.90 (C3,5(A)),122.30 (C4(A)), 136.13, 136.92 (C1(B), C1(C)), 133.30(C4(B),126.85(C3,5(C)), 128.85(C4(C)), 128.78, 128.68, 128.33 (C2,6(B), (C3,5(B), C2,6(C)), 197.59 (C=O), 27.58 (-CH_3); MS: *m/z*377 ($C_{23}H_{20}NO_2Cl$, M^+), 242 ($C_{15}H_{11}OCl$), 231 ($C_{13}H_{10}NOCl$), 216 ($C_{13}H_{11}NCl$), 131 ($C_9H_7O^+$), 111 ($C_6H_4Cl^+$), 91 (C_7H_7+).

3. Results and Discussion

3.1 *Experimental findings for 32CA reaction between **1** and **2***

32CA reaction between **1** and **2** afforded a diastereomeric mixture of *meta* cycloadducts **3** and **4** (Scheme 1) in the ratio 87:13 with the total yield of 75%. Structure elucidation was accomplished by spectroscopy (particularly NMR) and mass spectrometry. 300 MHz ^{1}H NMR spectrum of the major product

3 showed doublets at δ 5.58 ppm (J = 7.0 Hz) and δ 5.46 ppm (J = 9.2 Hz). A double doublet appeared at δ 4.03 ppm (J = 7.0, 9.2 Hz). The double doublet could be assigned to H4 of the isoxazolidine ring. For the minor cycloadduct **4**, two doublets appeared at δ 5.35 ppm (J = 10.3 Hz) and δ 6.51 ppm (J = 9.1 Hz) and the double doublet appeared at δ 4.97 ppm (J = 10.3, 9.1 Hz). Coupling constants of the two doublets rendered their respective assignments to H3 and H5 in **3** & **4** in accordance with our previously reported studies for 32CA reactions of nitrones to benzylidene acetophenone[40] and cinnamoyl piperidine.[41] The coupling constants supported 3,4-*trans*-4,5-*trans* stereochemistry in cycloadduct **3** [$J_{3,4}$ = 7.2 Hz and $J_{4,5}$ = 9.0 Hz in 3,4-*trans*-4,5-*trans* cycloadduct obtained from 32CA reaction of nitrone **1** to benzylidene acetophenone][40] and 3,4-*cis*-4,5-*trans* stereochemistry in cycloadduct **4** [$J_{3,4}$ = 10.1 Hz and $J_{4,5}$ = 9.5 Hz in 3,4-*cis*-4,5-*trans* cycloadduct obtained from 32CA reaction of nitrone **1** to benzylidene acetophenone].[40] ^{13}C NMR signals of ring C and mass spectral fragmentation peaks (see experimental section) supported the connectivity of C5 to the oxygen atom of the isoxazolidine ring.

3.2 *Analysis of the CDFT reactivity Indices and ELF topological analysis of the reactants*

Several theoretical studies devoted to 32CA reactions[15] have reported the analysis of DFT based global indices to characterize the feasibility of the reactions. Consequently, the electronic chemical potentials (μ), chemical hardness (η), electrophilicity (ω) and nucleophilicity (N) indices of nitrone **1** and benzylidene acetone **2** were computed and analyzed (Table 1). The electronic chemical potential μ of benzylidene acetone **2**, μ = −4.10 eV is only slightly lower than that of the nitrone **1**, μ = −3.80 eV, which indicates that transfer of electron density is unlikely to occur in either direction. These values predict a non-polar reaction between **1** and **2**. This is in complete agreement with the calculated global electron density transfer (GEDT[11]) computed at the transition states (TSs) (see section 3.3). As the reaction is predicted to be non-polar, the regioselectivity could not be predicted by analysis of two-centre or four center interactions by local reactivity indices, such as Fukui[42] or Parr functions.[43] Reagents **1** and **2** show almost similar electrophilicity ω of 1.96 eV(**1**) and 1.87 eV(**2**), which renders their classification as strong electrophiles according to the absolute scale of electrophilicity.[34] Nitrone **1** is classified as a strong nucleophile ($N > 3$ eV), while benzylidene acetone **2** as a moderate nucleophile ($N < 3$ eV).[15]

Table 1. B3LYP/6-31G(d) calculated electronic chemical potentials (μ), chemical hardness (η), electrophilicity (ω) and nucleophilicity (N) indices of the reactants in eV.

	μ	η	ω	N
1	−3.80	3.67	1.96	3.48
2	−4.10	4.49	1.87	2.78

The concept of Electron Localization Function (ELF) for atomic and molecular systems was introduced by Becke and Edgecombe,[13] followed by the outlining contribution of Silvi and Savin[14] in the use of ELF attractors for classification of chemical bonds. Domingo[8,9] correlated the electronic structures of the simplest three atom components (TACs) and their reactivities in 32CA reactions. Monosynaptic basin V(A) integrating 1e are associated with *pseudoradical center* at A, while V(A) integrating. 2e in a neutral molecule is associated with carbenoid *center* at A. TACs are classified as (1) Two *pseudoradical* centers: *Pseudodiradical* TAC *(-pdr type)*, (2) One *pseudoradical* center: *Pseudo(mono)radical* TAC *(-pmr type)* (3) One carbenoid *centre*: Carbenoid TAC (*cb- type*) (4) No *pseudoradical* or carbenoid *centre*: Zwitterionic TAC (*zw- type*)

ELF localization domains and basin attractor positions with the most significant valence basin population of reactants **1** and **2** are given in Figure 1. ELF topological analysis can provide the interpretation of Lewis's bonding model of a molecular system.[8] The proposed Lewis like structures of **1** and **2** is given in Scheme 3.

ELF topological analysis of nitrone **1** shows the presence of V(C3,N2) and V(N2,O1) disynaptic basins integrating at the populations of 3.93e and 1.30e, respectively which can be associated with underpopulated C3-N2 double bond and underpopulated N2-O1 single bond. V(O1) and V'(O1) monosynaptic basins integrating a total population of 5.95e can be associated with the lone pair electron density at oxygen atom O1 of **1**. Nitrone **1** has neither a *pseudoradical* center nor a carbenoid centre, allowing its classification as zwitterionic TAC (*zw- type*). TAC reactivity decreases in the order:[9,12] *pdr-type* > *pmr-type* ≈ *cb-type*>*zw-* type. *zw* type 32CA reactions are associated with high activation energies, which is also observed in the present study (see section 3.3). ELF topological analysis of **2** shows V(C4,C5) and V'(C4,C5) disynaptic basins integrating at a total population of 3.38e which can be associated with the underpopulated C4-C5 double bond. For styrene, V(C4,C5) and V'(C4,C5) disynaptic basins integrate at a total population of 3.50e.

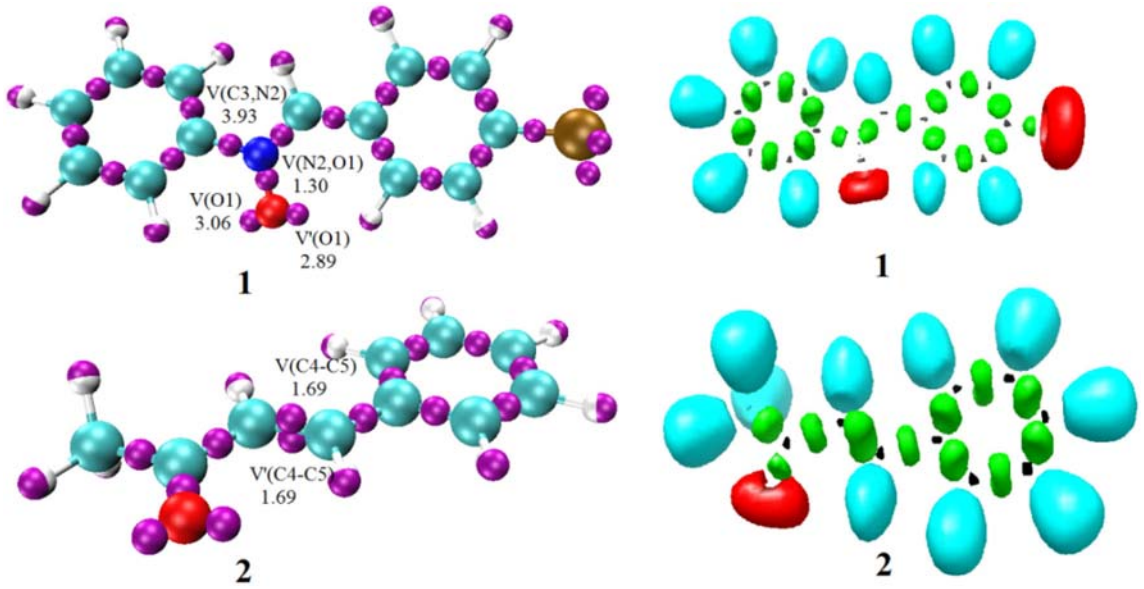

Figure 1. ELF localization domains [Isovalue: 0.79] and Basin attractor positions together with the most significant ELF valence basin populations for the reactant molecules. Attractors are shown by purple spheres, ELF valence basin population are given in average number of electrons, e. Protonated basins are shown in blue, disynaptic basins are shown in green, monosynaptic basins are shown in red and core basins are shown in black colours.

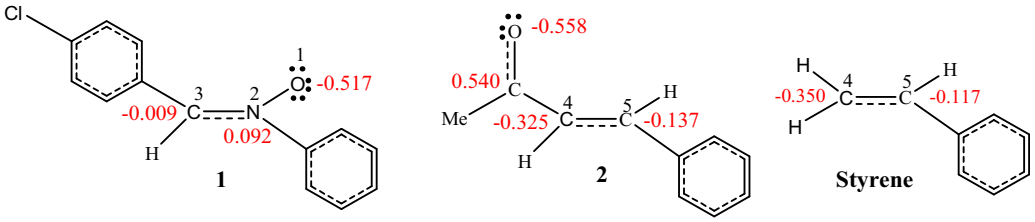

Scheme 3. Proposed Lewis-like structure of the reactants (based on ELF basin population) and calculated natural atomic charges (shown in red) are given in an average number of electrons, e.

Charge distribution of the reactants was analyzed through natural population analysis[31,32] (NPA). O1 of nitrone **1** is negatively charged by 0.517e, while nitrogen N2 and carbon C3 show negligible charges of 0.092e and 0.009e (Scheme 3). This framework of natural charges supports charge separation in TAC **1**, however, the charge separation is not in line with the Lewis bonding model. This indicates that the charge separation is not the outcome of resonance Lewis structure, but asymmetric electron density delocalization in the molecule due to the presence of different nuclei. C4 of Benzylidene acetone **2** and styrene shows the higher magnitude of negative charge than C5, owing to the presence of C5 phenyl substituent.

3.3 *Study of the energy profile associated with the 32CA reactions*

There are two possible regioisomeric channels, *ortho* and *meta* for 32CA reaction of nitrone **1** and benzylidene acetone **2**. *Ortho* approach is associated with the formation of O1-C4 and C3-C5 bonds, while the *meta channel* is associated with the formation of O1-C5 and C3-C4 bonds (Scheme 4). The *endo* and *exo* stereochemical approaches along these two regioisomeric channels can lead to four possible cycloadducts. The search for stationary points along these four reaction paths allowed locating and characterizing the reagents **1** and **2**, four TSs **TSmn**, **TSmx**, **TSon** and **TSox** along with the *endo*/*meta*, *exo*/*meta*, *endo*/*ortho* and *exo*/*ortho* approach modes and the corresponding cycloadducts **CAmn**, **CAmx, CAon** and **CAox** (Scheme 4). This 32CA reaction follows a *one-step* mechanism. The activation energies range from 80.1 (**TSmn**) to 95.7 (**TSox**) kJ mol^{-1} in the gas phase and from 88.4 (**TSmn**) to 103.4 (**TSox**) kJ mol^{-1} in toluene, with the reaction being exothermic in the range −20.4 to −41.7 kJ mol^{-1} in the gas phase and −12.1 to −31.0 kJ mol^{-1} in toluene. The most favorable reaction path of this kinetically controlled reaction is associated with the *meta/endo* approach

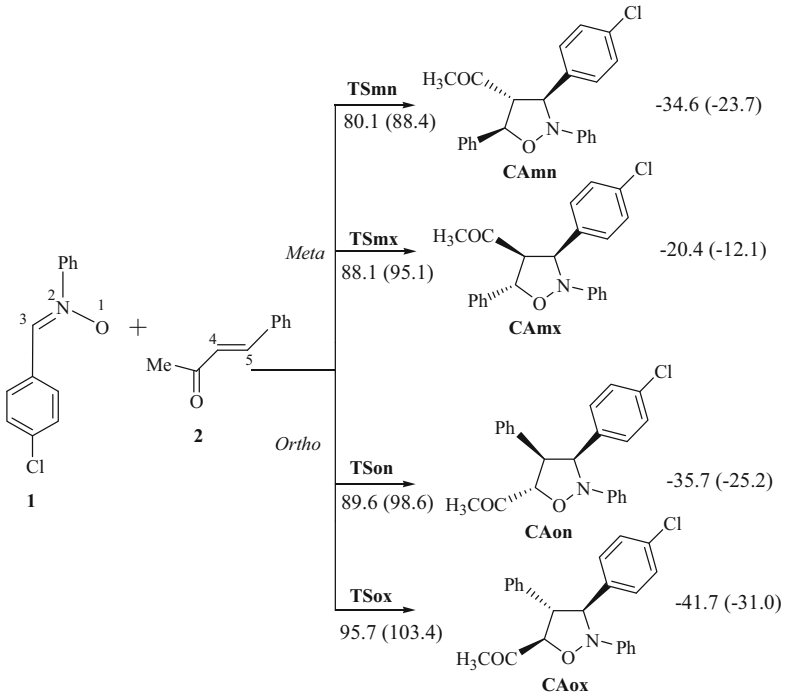

Scheme 4. Possible regio- and stereoisomeric pathways for 32CA reaction between **1** and **2**. Activation energies are given in kJ/mol. Activation energies in parenthesis are calculated in toluene solvent.

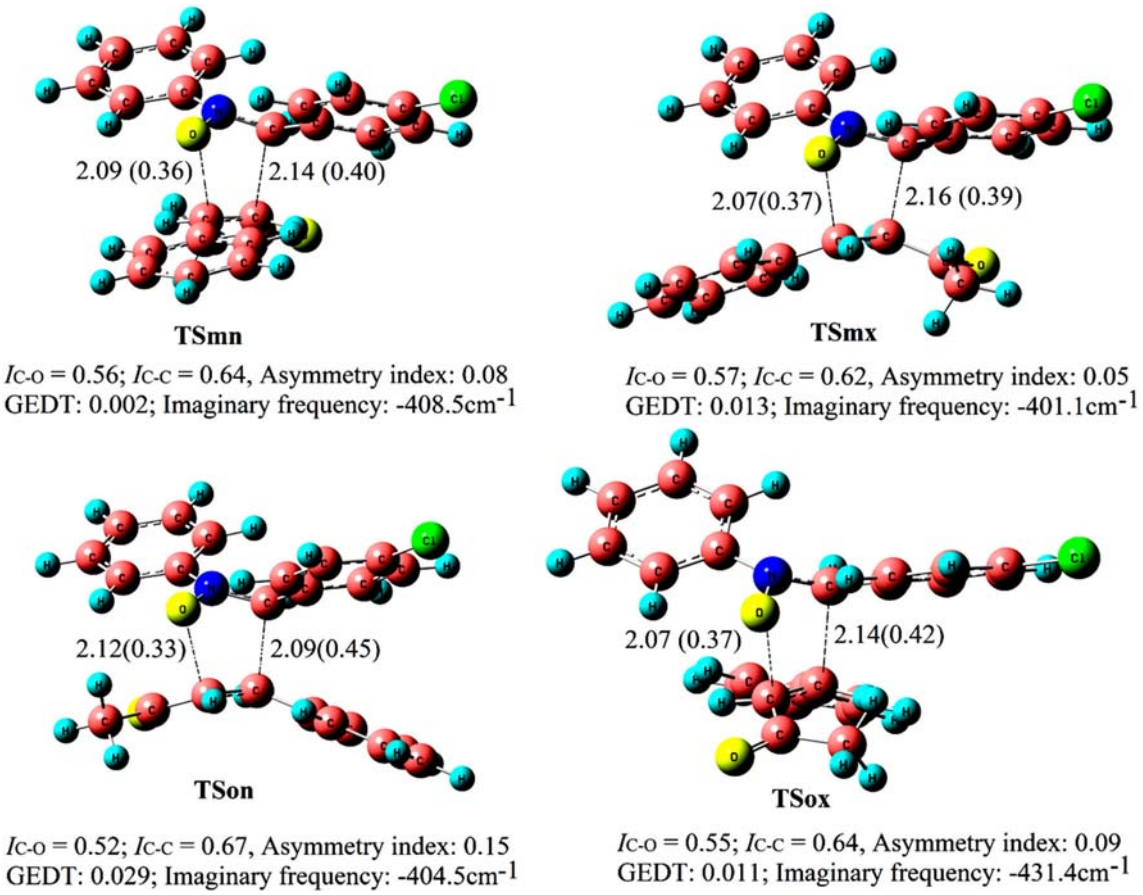

Figure 2. B3LYP/6-31G(d) optimized transition states for 32CA reaction of **1** and **2**. $I_{C\text{-}C}$ = 1- ($\{r^{TS}_{C-C}$ - $r^{P}_{C-C}\}/r^{P}_{C-C}$); $I_{C\text{-}O}$ = 1- ($\{r^{TS}_{C-O}$ - $r^{P}_{C-O}\}/r^{P}_{C-O}$); r^{TS} and r^{P} are the bond distances of TSs and cycloadducts; Asymmetry index,[46] Δa = $I_{C\text{-}C}$ - $I_{C\text{-}O}$.

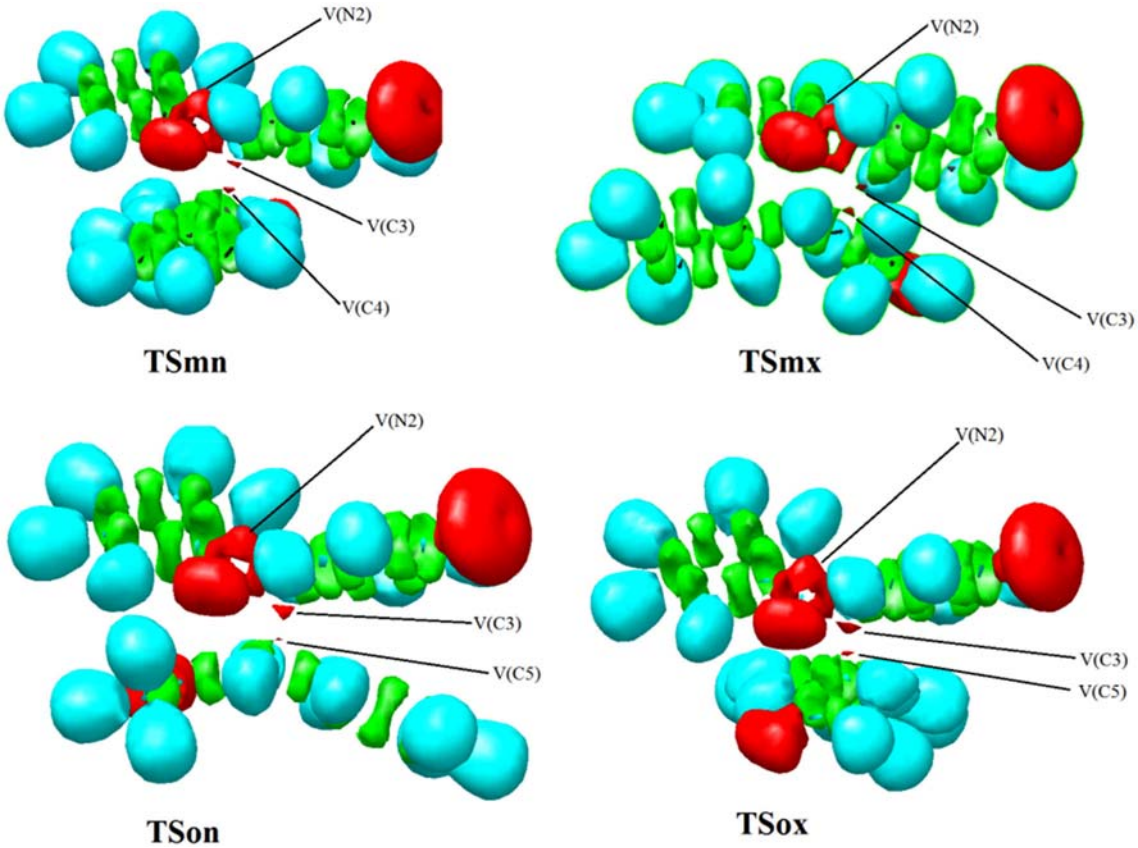

Figure 3. ELF localization domains [Isovalue: 0.79] the TSs. Protonated basins are shown in blue, disynaptic basins are shown in green, monosynaptic basins are shown in red and core basins are shown in black colours.

Table 2. ELF topological analysis at the TSs.

	V(O1)	V'(O1)	V(C3,N2)	V(N2,O1)	V(C4,C5)	V(N2)	V(C3)	V(C4)	V(C5)
TSmn	2.93	2.94	2.36	1.11	2.72	1.33	0.47	0.43	–
TSmx	2.93	2.95	2.31	1.10	2.69	1.32	0.45	0.45	–
TSon	2.91	2.92	2.18	1.14	2.66	1.24	0.60	–	0.39
TSox	2.89	2.94	2.27	1.13	2.71	1.34	0.56	–	0.40

Table 3. QTAIM parameters in [au] of (3,-1) critical points at the transition states in the regions associated with the generation of new C-C (CP1) and C-O (CP2) single bonds.

	CP1 (C3-C4)			CP2 (C5-O1)		
TS	ρ	$\nabla^2_{\rho(r_c)}$	$E_{\rho(r_c)}$	ρ	$\nabla^2_{\rho(r_c)}$	$E_{\rho(r_c)}$
TS1	0.068	0.029	−0.018	0.062	0.117	−0.007
TS2	0.066	0.032	−0.017	0.064	0.117	−0.008
TS3	0.076	0.014	−0.023	0.059	0.117	−0.006
TS4	0.069	0.025	−0.019	0.065	0.121	−0.008

mode, yielding the experimental isoxazolidine **3** *via* **TSmn**. The high activation energy of 80.1 kJ mol^{-1} is in agreement with the *zw-type* character. This reaction is completely regioselective with relative energy of **TSmn** less than the *ortho* TSs by 9.5 and 15.6 kJ/mol in the gas phase and 10.2 and 15.0 kJ/mol in toluene. In our previous studies,[44,45] we have observed that 32CA reaction of *C*,*N*-disubstituted nitrones to ethyl vinyl ketone and methyl crotonate also follow *one-step* mechanism and show energy barriers of 40.6 kJ/mol and 57.8 kJ/mol, respectively along with the favoured *ortho/exo* and *meta/endo* pathways, which are lower than that calculated for the present study.

Optimized geometries of the TSs are given in Figure 2. The calculated bond orders of the forming C-C bonds are higher than that of C-O bonds in each case. Finally, the polar character was evaluated by GEDT calculations at the TSs. GEDT values at the

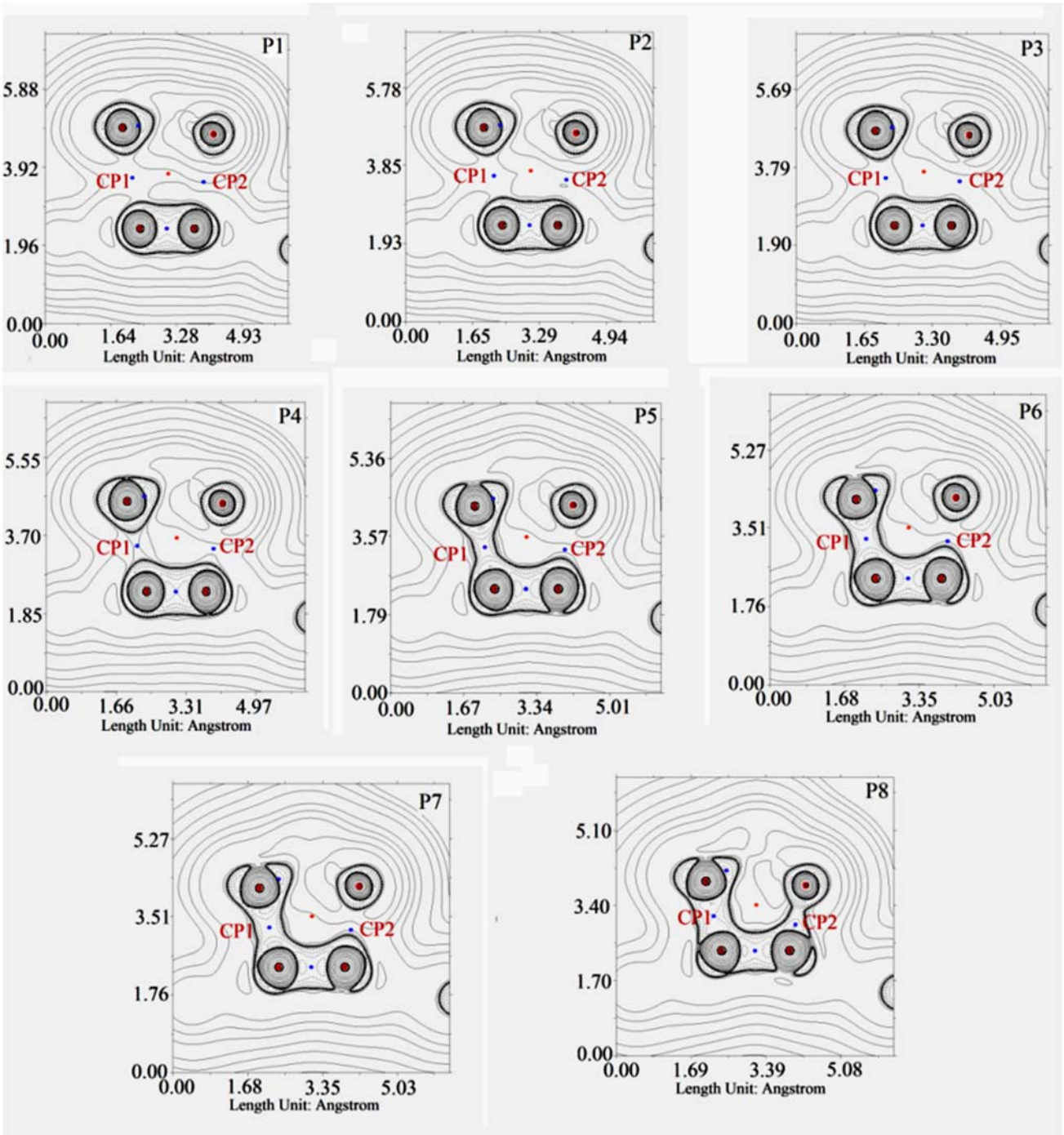

Figure 4. Representations of the contour line maps of the Laplacian of the electron density along *endo*/*meta* pathway of 32CA reaction between **1** and **2** at selected IRC coordinate points along the reaction pathway on the molecular plane defined by atoms for C3-C4 (C-C) and C5-O1 (C-O) bond formation, CP1 (3,-1) and CP2 (3,-1) critical points respectively are marked in the representation.

TSs vary from 0.002e to 0.029e. This is indicative of the non-polar character, which is supported by the minimal difference between electronic chemical potentials of **1** and **2** (Table 1). Generally speaking, non-polar 32CA reactions are associated with high activation energies, which is also observed in the present study with the enone system.

3.4 *ELF topological analysis at the transition states*

ELF localization domains at the TSs are given in Figure 3, with the most significant valence basin populations listed in Table 2. Topological analysis of the ELF of TSs **TSmn**, **TSmx**, **TSon** and **TSox** show

the presence of V(O1) and V'(O1) monosynaptic basins with total integrating population of 5.83-5.88 e (Table 2), which can be associated with the non-bonding electron density at the oxygen atom. Disynaptic V(C3,N2) basin integrating at 2.18-2.36 e can be associated with the C3-N2 bond that has experienced depopulation and hence ruptures along the reaction course while proceeding from the reactants to the TSs. V(N2) monosynaptic basin can be associated with the lone pair electron density at N2 nitrogen.

C4-C5 bond rupture is also evident from the disynaptic V(C4,C5) basin integrating at 2.66-2.72e. TSs also show the presence of monosynaptic V(C3) basin less than 1e which can be associated with the formation of *pseudoradical* centre at C3 carbon. *Meta* TSs, **TSmn** & **TSmx** show the presence of monosynaptic basins at C4, while *ortho* TSs, **TSon** & **TSox** show the presence of monosynaptic basins at C5, which can be associated respectively with the formation of *pseudoradical* centers at C4 and C5.

3.5 *Identification of the atomic interactions at the interatomic bonding regions*

Bader's **Q**uantum **T**heory of **A**toms **i**n **M**olecules[16–18] (QTAIM) has been widely used to unravel the covalent and non-covalent interactions in molecular systems. The Laplacian of electron density ∇^2 plays a significant role to characterize the covalent/non-covalent interactions present in molecular systems. We have recently applied[44] this QTAIM concept to characterize the nature of bonding in 32CA reactions of nitrone to ethyl vinyl ether. The calculated QTAIM parameters at the (3,-1) bond critical point (BCP) at the TSs are given in Table 3 with contour line map of the Laplacian of electron density at the selected IRC points along the *endo*/*meta* pathway represented in Figure 4. Positive Laplacian at the BCPs (Table 3) indicate that the formed bond at the TSs is non-covalent in nature and a small amount of electron density ρ is involved in the bonding.

NCI plot program was introduced in 2011 by Yang and co-workers[19] to plot and visualize the bonded and non-bonded non-covalent gradient isosurfaces, defined by the sign of λ_2,[16–18] a component of the Laplacian of electron density.[16–18] NCI plots of **TSmn** is given in Figure 5. For **TSmn**, the non-covalent attractive bonded overlap (blue portions) and non-bonded overlap (red portions) are present between O1 & C5, and also between C3 & C4. This indicates the presence of non-covalent interaction at the C3-C5 & C5-O1 interatomic bonding region, which agrees with the calculated positive Laplacian of electron density (Table 3).

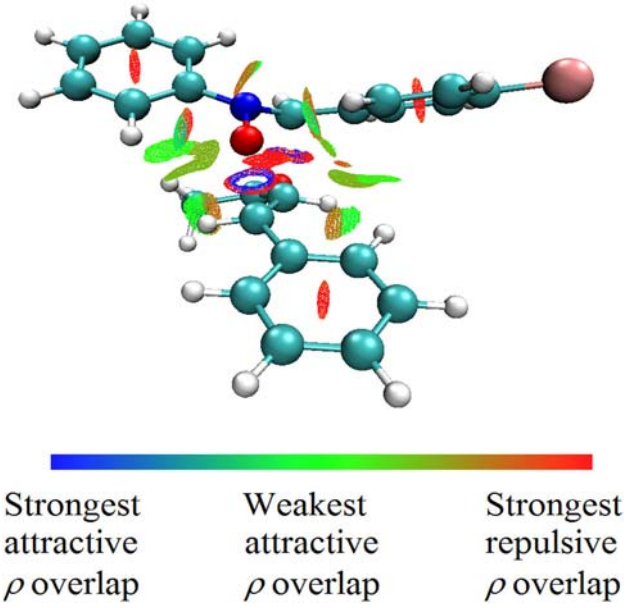

Figure 5. B3LYP/6-31G(d) calculated Non-covalent interactions (NCI) gradient isosurfaces of reduced density gradient [as values of sign $(\lambda_2)\rho$] at **TSmn**. Surfaces are coloured in the [−0.04 (blue), 0.02 (red)] a.u. (Isosurfaces = 0.5 a.u.).

4. Conclusions

[3 + 2] cycloaddition reaction of *C*-(4-chlorophenyl)-*N*-phenyl nitrone to benzylidene acetone is non-polar zwitter-ionic (*zw*) type and proceeds through *one-step* mechanism with asynchronous TSs. The reaction is regioselective with *endo*/*meta* pathway predicted as the favored mode of approach with a high activation energy barrier of 80.1 kJ/mole, in line with its *zw-type* character. The origin of high activation energy barrier is the energy required for the rupture of C-C double bond to form *pseudoradical* centers and new C-C and C-O single bonds of the isoxazolidine adduct are generated through the coupling of these *pseudoradical* centers. This 32CA reaction involves non-covalent interactions between the reacting nuclei at the TSs, as evident from the positive Laplacian of electron density and visualization of gradient isosurfaces in the non-covalent interaction (NCI) plot.

Supplementary Information (SI)

(1) 300 MHz ^{1}H NMR spectra of the crude reaction mixture (2) 300 MHz ^{1}H NMR spectrum of cycloadducts **3** and **4** (3) 75.5 MHz ^{13}C NMR spectrum of cycloadducts **3** and **4** (4)

Mass spectrum of cycloadduct **3** (5) Cartesian Coordinates and optimized energies of all reactants, products and transition states (6) ELF basin populations along *endo/meta* pathway are available at www.ias.ac.in/chemsci.

Acknowledgements

One of the authors N. Acharjee, is thankful to Professor Manas Banerjee (Retired), University of Burdwan, West Bengal, India for kind cooperation and University of Calcutta for experimental facilities.

References

1. Grigor'ev I A 2007 In *Nitrile Oxides, Nitrones, and Nitronates in Organic Synthesis* H Feuer (Ed.) (Wiley: Hoboken, New Jersey) p. 129
2. Jones R C F and Martin J N 2002 In *Synthetic Application of 1,3-Dipolar Cycloaddition Chemistry Toward Heterocycles and Natural Products* A Padwa and W H Pearson (Eds.) (Wiley: New York) p.1
3. Chiacchio M A, Giofrè S V, Romeo R, Romeo G and Chiacchio U 2016 Isoxazolidines as Biologically Active Compounds *Curr. Org. Syn.* **13** 726
4. Romeo G, Chiacchio U, Corsaro A and Merino P 2010 Chemical Synthesis of Heterocyclic-Sugar Nucleoside Analogues *Chem. Rev.* **110** 3337
5. Gothelf K V and Jørgensen K A 1998 Asymmetric 1,3-Dipolar Cycloaddition Reactions *Chem. Rev.* **98** 863
6. Zhang Q Y Z, Jia Z, Yang C, Zhang L and Luo S 2019 Asymmetric 1,3-Dipolar Cycloaddition Reactions of Enones by Primary Amine Catalysis *Asian J. Org. Chem.* **8** 1049
7. Fukui K, Yonezawa T and Shingu H 1952 A Molecular Orbital Theory of Reactivity in Aromatic Hydrocarbons *J. Chem. Phys.* **20** 722
8. Domingo L R 2016 Molecular Electron Density Theory: A Modern View of Reactivity in Organic Chemistry *Molecules* **21** 1319
9. Gutiérrez M R and Domingo L R 2019 Unravelling the Mysteries of the [3 + 2] Cycloaddition Reactions *Eur. Jour. Org. Chem.* 267
10. Domingo L R, Gutiérrez M R- and Pérez P 2017 How does the global electron density transfer diminish activation energies in polar cycloaddition reactions? A Molecular Electron Density Theory study *Tetrahedron* **73** 1718
11. Domingo L R 2014 A new C–C bond formation model based on the quantum chemical topology of electron density *RSC Adv.* **4** 32415
12. Domingo L R, Gutiérrez M R- and Pérez P 2018 A Molecular Electron Density Theory Study of the Reactivity and Selectivities in [3 + 2] Cycloaddition Reactions of C,N-Dialkyl Nitrones with Ethylene Derivatives *J. Org. Chem.* **83** 2182
13. Becke A D and Edgecombe K E 1990 A simple measure of electron localization in atomic and molecular systems *J. Chem. Phys.* **92** 5397
14. Silvi B and Savin A 1994 Classification of chemical bonds based on topological analysis of electron localization functions *Nature* **371** 683
15. Domingo L R, Gutiérrez M R and Pérez P 2016 Applications of the Conceptual Density Functional Theory Indices to Organic Chemistry Reactivity *Molecules* **21** 748
16. Bader R F W 1990 *Atoms in Molecules: A Quantum Theory* (Oxford: Clarendon Press)
17. Kumar P S V, Raghavendra V and Subramanian V 2016 Bader's Theory of Atoms in Molecules (AIM) and its Applications to Chemical Bonding *J. Chem. Sci.* **128** 1527
18. Bader R F W and Essén H 1984 The characterization of atomic interactions *J. Chem. Phys.* **80** 1943
19. García J C-, Johnson E R, Keinan S, Chaudret R, Piquemal J -P, Beratan D N and Yang W 2011 NCIPLOT: A Program for Plotting Noncovalent Interaction Regions *J. Chem. Theory Comput.* **73** 625
20. Becke A D 1988 Density-functional exchange-energy approximation with correct asymptotic behavior *Phys. Rev. A* **38** 3098
21. Lee C, Yang W and Parr R G 1988 Development of the Colle-Salvetti correlation-energy formula into a functional of the electron density *Phys. Rev. B* **37** 785
22. Domingo L R, Aurell M J and Pérez P 2015 A mechanistic study of the participation of azomethine ylides and carbonyl ylides in [3 + 2] cycloaddition reactions *Tetrahedron* **71** 1050
23. Jasiński R 2015 In the searching for zwitter ionic intermediates on reaction paths of [3 + 2] cycloaddition reactions between 2,2,4,4-tetramethyl-3-thiocyclobutanone S-methylide and polymerizable olefins *RSC Adv.* **5** 101045
24. Kącka- Zych A, Domingo L R, Gutiérrez M R and Jasiński R 2017 Understanding the mechanism of the decomposition reaction of nitroethyl benzoate through the Molecular Electron Density Theory *Theor. Chem. Acc.* **136** 129
25. González C and Schlegel H B 1990 Reaction path following in mass-weighted internal coordinates *J. Phys. Chem.* **94** 5523
26. González C and Schlegel H B 1991 Improved algorithms for reaction path following: Higher-order implicit algorithms *J. Chem. Phys.* **95** 5853
27. Tomasi J and Persico M 1994 Molecular Interactions in Solution: An Overview of Methods Based on Continuous Distributions of the Solvent *Chem. Rev.* **94** 2027
28. Simkin B I A and Sheikhet I I 1995 *Quantum chemical and statistical theory of solutions—Computational approach* (London, UK: Ellis Horwood)
29. Cossi M, Barone V, Cammi R and Tomasi J 1996 Ab initio study of solvated molecules: a new implementation of the polarizable continuum model *Chem. Phys. Lett.* **255** 327
30. Barone V, Cossi M and Tomasi J 1998 Geometry optimization of molecular structures in solution by the polarizable continuum model *J. Comput. Chem.* **19** 404
31. Reed A E, Weinstock R B and Weinhold F 1985 Natural Population Analysis *J. Chem. Phys.* **83** 735

32. Reed A E, Curtiss L A and Weinhold F 1988 Intermolecular interactions from a natural bond orbital, donor-acceptor viewpoint *Chem. Rev.* **88** 899
33. Geerlings P, De Proft F and Langenaeker W 2003 Conceptual Density Functional Theory *Chem. Rev.* **103** 1793
34. Domingo L R, Aurell M J, Perez P and Contreras R 2002 Quantitative Characterization of the Global Electrophilicity Power of Common Diene/Dienophile Pairs in Diels-Alder Reactions *Tetrahedron* **58** 4417
35. Gaussian 03, Revision D.01, Frisch M J, Trucks G W, Schlegel H B, Scuseria G E, Robb M A, Cheeseman J R, Montgomery Jr JA, Vreven T, Kudin K N, Burant J C, Millam J M, Iyengar S S, Tomasi J, Barone V, Mennucci B, Cossi M, Scalmani G, Rega N, Petersson GA, Nakatsuji H, Hada M, Ehara M, Toyota K, Fukuda R, Hasegawa J, Ishida M, Nakajima T, Honda Y, Kitao O, Nakai H, Klene M, Li X, Knox J E, Hratchian H P, Cross J B, Bakken V, Adamo C, Jaramillo J, Gomperts R, Stratmann R E, Yazyev O, Austin A J, Cammi R, Pomelli C, Ochterski J W, Ayala P Y, Morokuma K, Voth G A, Salvador P, Dannenberg J J, Zakrzewski V G, Dapprich S, Daniels A D, Strain M C, Farkas O, Malick D K, Rabuck A D, Raghavachari K, Foresman J B, Ortiz J V, Cui Q, Baboul A G, Clifford S, Cioslowski J, Stefanov B B, Liu G, Liashenko A, Piskorz P, Komaromi I, Martin R L, Fox D J, Keith T, Al-Laham M A, Peng C Y, Nanayakkara A, Challacombe M, Gill P M W, Johnson B, Chen W, Wong M W, Gonzalez C and Pople J A, Gaussian, Inc, Wallingford CT, 2004
36. Lu T and Chen F 2012 Multiwfn: A multifunctional wavefunction analyzer *J. Comp. Chem.* **33** 580
37. Humphrey W, Dalke A and Schulten K 1996 VMD: visual molecular dynamics *J. Mol. Graphics.* ***14.1*** 33
38. Pettersen E F, Goddard T D, Huang C C, Couch G S, Greenblatt D M, Meng E C and Ferrin T E 2004 UCSF Chimera–a visualization system for exploratory research and analysis *J. Comput. Chem*. **25** 1605
39. Drake N L and Allen P Jr. 1923 Benzalacetone *Org. Synth.* **3** 17
40. Acharjee N, Banerji A and Prangé T 2010 DFT study of 1,3-dipolar cycloadditions of C,N-disubstituted aldonitrones to chalcones evidenced by NMR and X-ray analysis *Monatsh. Chem.* **141** 1213
41. Banerji A, Maiti K K, Haldar S, Mukhopadhyay C, Banerji J, Prange´ T and Neuman A 2000 1,3-Dipolar Cycloadditions VI [1].Structure and Conformation of Cycloadducts from Reactions of C-Aryl-N-phenyl nitrones with Substituted Cinnamic Acid Amides *Monatsh. Chem.* **131** 901
42. Yang W and Mortier W J 1986 The use of global and local molecular parameters for the analysis of the gas-phase basicity of amines *J. Am. Chem. Soc.* **108** 5708
43. Domingo L R, Pérez P and Sáez J A 2013 Understanding the local reactivity in polar organic reactions through electrophilic and nucleophilic Parr functions *RSC Adv.* **3** 1486
44. Domingo L R and Acharjee N 2018 [3 + 2] Cycloaddition Reaction of C-Phenyl-N-methyl Nitrone to Acyclic-Olefin-Bearing Electron-Donating Substituent: A Molecular Electron Density Theory Study *Chem. Select* **3** 8373
45. Acharjee N and Banerji A 2011 DFT interpretation of 1,3-dipolar cycloaddition reaction of C,N-diphenyl nitrone to methyl crotonate in terms of reactivity indices, interaction energy and activation parameters *Comput. Theo. Chem.* **967** 50
46. Jasiński R, Wąsik K, Mikulskaa M and Barański A 2009 A DFT study on the (2 + 3) cycloaddition reactions of 2-nitropropene-1 with Z-C, N-diarylnitrones *J. Phys. Org. Chem.* **22** 717